

Density functional theory based molecular dynamics study of hydration and electronic properties of aqueous La^{3+}

Cyril Terrier,^{1,a)} Pierre Vitorge,^{1,a)} Marie-Pierre Gaigeot,^{1,b)} Riccardo Spezia,^{1,c)} and Rodolphe Vuilleumier^{2,c)}

¹Laboratoire Analyse et Modélisation pour la Biologie et l'Environnement, CNRS UMR 8587, Université d'Evry Val d'Essonne, Boulevard F. Mitterrand, 91025 Evry Cedex, France

²Département de Chimie, Ecole Normale Supérieure, UMR CNRS 8640 PASTEUR, 24 rue Lhomond, F-75231 Paris Cedex 05, France

(Received 26 February 2010; accepted 16 June 2010; published online 28 July 2010)

Structural and electronic properties of La^{3+} immersed in bulk water have been assessed by means of density functional theory (DFT)-based Car–Parrinello molecular dynamics (CPMD) simulations. Correct structural properties, i.e., La(III)-water distances and La(III) coordination number, can be obtained within the framework of Car–Parrinello simulations providing that both the La pseudopotential and conditions of the dynamics (fictitious mass and time step) are carefully set up. DFT-MD explicitly treats electronic densities and is shown here to provide a theoretical justification to the necessity of including polarization when studying highly charged cations such as lanthanoids(III) with classical MD. La^{3+} was found to strongly polarize the water molecules located in the first shell, giving rise to dipole moments about 0.5 D larger than those of bulk water molecules. Finally, analyzing Kohn–Sham orbitals, we found La^{3+} empty 4*f* orbitals extremely compact and to a great extent uncoupled from the water conduction band, while the 5*d* empty orbitals exhibit mixing with unoccupied states of water. © 2010 American Institute of Physics. [doi:10.1063/1.3460813]

I. INTRODUCTION

In the past decades, a great amount of work has been devoted to the understanding of the hydration structure of metal cations in liquid water, using both experimental and theoretical approaches.^{1–5} Among these metal cations, lanthanoids play an interesting role since they have the same charge (3+) but two coordination structures as a function of their atomic number: light lanthanoids possess a ninefolded structure, while heavier lanthanoids have an eightfolded arrangement.^{6,7} Recently, experimental and theoretical studies have focused on a fine determination of first shell polyhedra.^{8–10} In particular, different classical interaction potentials were developed at this aim. A class of it includes polarization that was found to be a key physical effect to correctly address hydration behavior.^{11–15} Another class of effective potentials was obtained for Nd(III), Gd(III), and Yb(III) from fitting *ab initio* calculations in the polarizable continuum model.^{10,16}

As a price to pay, classical simulations do not provide any information on the metal electronic structure and relationship with its environment (solvent and ligands) and cannot take into account chemical reactivity as hydrolysis¹⁷ or ligand binding. In groundwaters as studied in the framework

of nuclear storage, lanthanoid cations are generally liganded, for instance, with carbonate^{18,19} or sulfate ions,²⁰ and, as already observed for the metal aqueous hydration, the number of ligands can depend on the metal atomic number.²¹ The investigation of such lanthanoid-ligand ionic complexes with a surrounding solvent using classical molecular dynamics simulations would require a large parameterization effort but in any case would not be suitable to study the breaking of covalent bonds as for hydrolysis. Any theoretical attempt in these directions thus requires a full *ab initio* representation of lanthanoid metal ions that will be able to take care of the metal immersed in aqueous solution as well as its complexation and chemical reactivity in different environments.

Density functional theory (DFT)-based molecular dynamics (MD), for instance, in the Car–Parrinello molecular dynamics (CPMD) scheme,²² is a well suited method to treat reactivity and complexation in solution, and it has been successfully employed to describe solvation of different cations in liquid water^{23–28} and to study metal complexation in solution.^{29,30} A key aspect for a correct description of the metal-solvent or metal-ligand potential energy surface is the choice of the functional and of the metal pseudopotential. For on-the-fly DFT dynamics, only generalized gradient approximation functionals are computationally doable, and the Becke–Lee–Yang–Parr (BLYP) functional^{31,32} has been shown to satisfactorily describe the structure of liquid water^{33,34} as well as the solvation of a variety of ions in aqueous solution.^{35–40} The pseudopotentials are used to reduce the number of explicit electrons (and to use a reasonable cutoff radius in the plane wave expansion), but we have to pay the

^{a)}Also at: CEA Saclay, DEN/DPC/SECR/LSRM, 91991 Gif Sur Yvette, France.

^{b)}Also at: Institut Universitaire de France (IUF), 103 Blvd. St. Michel, 75005 Paris, France.

^{c)}Authors to whom correspondence should be addressed. Electronic addresses: riccardo.spezia@univ-evry.fr and rodolphe.vuilleumier@ens.fr. FAX: (+33) 1 69 47 76 55.

price of finding the good form and parameters. Three such pseudopotentials will be tested in the present work.

Hydration is a good reference test case for different reasons. (i) Many data from simulations and experiments are available. (ii) Explicit modeling of hydration is a first step in the investigation of the aqueous chemistry of these ions at the molecular level, which is our primary interest. Note that DFT-MD can be also applied to characterize the hardness and softness of cations.⁴¹ La^{3+} is generally considered as a hard cation, and the characterization of its hardness in water from an electronic structure point of view is of interest for its subsequent aqueous chemistry. (iii) The metal-water interaction is generally more difficult to describe than metal-ligand interactions, as the results are generally more sensible to DFT performances and simulation conditions. (iv) Last but not least, La^{3+} hydration study via DFT-MD will provide useful information on the nature of La^{3+} -water interactions and on the role of f orbitals, as La^{3+} can be seen to be at the edge between d and f elements in the series.

The hydration structure of La^{3+} is experimentally well known. The La–O distance was found in the 2.54–2.56 Å range by recent extended X-ray absorption fine structure (EXAFS) experiments,⁸ confirming the earlier x-ray diffraction experiments^{42–44} that gave a 2.48–2.58 Å range. Concerning the coordination number (CN), the question was a subject of a debate from experimental side. In fact, early experiments^{42–45} provided a large range of possible CNs, from 8 to 12. Finally, in the past years, they converged to the value of 9, which should be considered nowadays as the correct CN for La^{3+} hydration,^{8,46,47} and we will use this result as reference to compare our simulations. Further, La^{3+} hydration can be correctly described by one structure only, CN=9, because of rare self-exchange events^{11,48} and also because other intermediate structures are not stable enough to be crucial for EXAFS or XRD interpretation.

Few *ab initio* or DFT-based MD of aqueous lanthanoids have been reported in the literature. Rode and co-workers used a mixed quantum mechanics/molecular mechanics (QM/MM) MD approach to investigate La(III) hydration, but results are not in full agreement with experiments as they provide a too long La–O first shell distance of 2.65 Å and consequently an overcoordinated ion with CN=9.5.⁴⁹ Two main investigations using DFT-based molecular dynamics have been reported in the literature, on Gd(III) (Ref. 50) and La(III),⁵¹ the last one employing a biased metadynamics sampling. Note that the Gd(III) study reported a stable coordination number of eight that appears to be too small in the light of recent experimental data.⁸ The experimental value very likely arises from the statistical coexistence of CN=8 and CN=9 in the solution via an interchange that occurs in a time scale larger than sampled by the CPMD simulations.⁹ On the other hand, a Gd(III)-O distance of 2.37 Å is compatible with the different experimental data,^{1,8,52,53} although on the lower side of the experimental range. This probably reflects the use of a Vanderbilt ultrasoft pseudopotential with a $[\text{Xe}]4f^1$ core configuration with f electrons included in the core. The metadynamics study of aqueous La^{3+} by Ikeda *et al.*⁵¹ explored different possible CNs, finding CN=8 and CN=8.5 few kcal/mol lower in free energy with respect to

CN=9. Finally, CPMD simulations were found to satisfactorily address the behavior of La^{3+} in a highly concentrated (14M) lithium chloride solution.⁵⁴

Not constrained DFT-MD simulations able to reproduce La^{3+} hydration properties are thus still missing. The present work aims at filling that gap in order to be able of using DFT-MD to study chemical reactivity. To that end, we have built three different La pseudopotentials to be combined with the BLYP functional. With the correct choice of pseudopotential and employing a small enough fictitious mass that commits the system as close as possible to the true Born–Oppenheimer hypersurface, we are able to reproduce the correct La–O distance and CN=9 with DFT-based Car–Parrinello dynamics. As a first application, we provide here information on the polarization induced to the surrounding solvent molecules by this highly charged La(III) ion and on the La^{3+} ion itself and on the electronic structure of the system.

The outline of the remainder of the text is as follows. In the next section, we describe the simulation setup and the data analysis procedure. Section III describes structural results, while Sec. IV deals with La^{3+} electronic properties. We summarize and conclude in Sec. V.

II. COMPUTATIONAL DETAILS

A. Car–Parrinello molecular dynamics

All CPMD calculations consist in one La^{3+} ion and 64 water molecules located in a cubic box of 12.43 Å edge so as to reproduce the water density at 300 K. Periodic boundary conditions were applied in order to mimic bulk conditions. The electronic structure of the valence electrons was described with DFT/BLYP functional,^{31,32} and the wave function was expanded in plane waves with an energy cutoff of 110 Ry. Note that more usual values are generally in the range of 60–80 Ry, and the relatively high value employed in the present work is needed to ensure a proper energy convergence (see text afterward). For the same reason, the fictitious mass used for the propagation of the electronic wave function has been chosen to 150 a.u., which is low in comparison to usual values of the literature (generally in the range of 400–700 a.u.). With that choice, the wave function is therefore able to adiabatically follow the Born–Oppenheimer surface much more easily. Note that these two requirements make our CPMD simulations more computationally expensive in comparison with other simulations of metal cations in bulk water from the literature.

Inherent to the use of a plane wave basis set, only valence electrons were considered, and pseudopotentials were thus employed for the electron-nuclei interaction. Medium soft norm-conserving pseudopotentials of the Troullier–Martins (TM) type were used here for all atoms.⁵⁵ These numerical pseudopotentials are obtained by fitting coefficients of a set of polynomials given reference, all electrons, atomic orbitals, and cutoff radii for the pseudopotential range. For lanthanum, we have generated here three different TM pseudopotentials for the description of the La^{3+} ion. These pseudopotentials differ in the number of core states and in the electronic state of isolated lanthanum taken as

TABLE I. Details on pseudopotentials.

	PP1	PP2	PP3
Number of valence electrons	11	11	3
Reference configuration	$5s^2 5p^6 5d^0 4f^0$	$5s^2 5p^6 5d^1 4f^0$	$6s^0 6p^0 5d^0 4f^0$
Nonlinear core corr.	No	No	Yes
Cutoff radii (a.u.)	1.36, 1.54, 2.03, 1.50	1.36, 1.54, 2.08, 1.50	3.18, 3.69, 2.03, 1.50

reference to fit the numerical TM pseudopotentials. The first pseudopotential (PP1) is a semicore potential where the $5s$ and $5p$ electrons are not included in the core, and the La(III) oxidation state was considered as reference electronic configuration. This leaves only eight semicore electrons, and the pseudoatom has a configuration $5s^2 5p^6 5d^0 4f^0$. This is the electronic configuration of La(III) solvated in water, and we thus expect that this pseudopotential leads to a correct description of the lanthanum orbitals in this situation. The cutoff radii (in a.u.) for the TM scheme are $R(5s)=1.36$, $R(5p)=1.54$, $R(5d)=2.03$, and $R(4f)=1.50$, chosen so as to reproduce the exact atomic orbitals up to the region of the outer maximum. The Kleinman–Bylander⁵⁶ semilocal scheme has been applied with p taken as the local channel in the simulation.

The second pseudopotential generated (PP2) is similar to PP1, but a different reference state was chosen. For PP2, the reference electronic configuration was the oxidation state La(II): $5s^2 5p^6 5d^1 4f^0$. The aim is to test the influence of this reference state on the end result, thus testing the transferability of these pseudopotentials for heavy metals from one oxidation state [here La(II) taken as reference] to another [La(III) for solvated La³⁺]. The cutoff radii for PP2 are (in a.u.) $R(5s)=1.36$, $R(5p)=1.54$, $R(5d)=2.08$, and $R(4f)=1.50$, respectively, very similar to PP1. The same semilocal scheme as for PP1 was applied.

Finally, as a third test, we generated a third pseudopotential (PP3) with again La(III) as reference state for the fit of the parameters but with a different choice of core-orbitals. This third pseudopotential (PP3) is not a semicore pseudopotential as PP1 and PP2 are but includes $5s$ and $5p$ orbitals in the core, and the valence orbitals used to construct PP3 are thus $6s$, $6p$, $5d$, and $4f$ orbitals. Since for heavy metals there is a spatial overlap between the core and the valence shell, which prompted us in generating semicore pseudopotentials, nonlinear core corrections are however employed with PP3. With La(III) oxidation state taken as reference, the reference configuration is $6s^0 6p^0 5d^0 4f^0$. The corresponding cutoff radii are (in a.u.) $R(6s)=3.18$, $R(6p)=3.69$, $R(5d)=2.03$, and $R(4f)=1.50$, respectively. Here again the Kleinman–Bylander semilocal scheme was used with $l=p$ as the local channel. Details for the three pseudopotentials are summarized in Table I.

For the three simulations, the total number of electrons is determined such that the total charge is +3. For both PP1 and PP2, La contributes eight electrons to this total number, while it contributes no electrons for PP3 as all valence states are empty in this case. For the three pseudopotentials, the final lanthanum electronic configuration is $5d^0 4f^0$ as expected for La(III) (discussed later). All Car–Parrinello simu-

lations were carried out with the program package CPMD (Ref. 57) in the NVT ensemble using the Nosé–Hoover thermostat^{58–60} with 300 K as target temperature. Initial structures were obtained from classical molecular dynamics equilibration using our polarizable potential.¹¹ The system was further re-equilibrated via 1 ps CPMD with initial velocities obtained from a Maxwell distribution centered on 300 K. Car–Parrinello data were then collected over 30 ps of simulation runs. Since we used a very small fictitious electron mass of 150 a.u., we also used a small time step of 2 a.u.

B. Data analyses

Structural analyses of the hydration patterns of the La(III) ion were done using standard radial distribution functions (RDFs) and coordination numbers (CNs). CNs are obtained through the integration of RDFs between r_{\min} and r_{\max} , with $r_{\min}=0$ and r_{\max} corresponds to the first minimum of RDF for first shell CN (CN⁽¹⁾), and $r_{\min}=r_{\max}$ used for CN⁽¹⁾ and r_{\max} corresponds to the second minimum of RDF for second shell CN (CN⁽²⁾). Radial distribution functions are complemented with angular distribution functions: (i) O–La–O angle formed by the La ion and two oxygens from its first hydration shell, (ii) θ the angle formed by the La–O vector (again O from first hydration shell) and the vector sum of the two O–H bonds [see Fig. 4(b)], and (iii) tilt angle formed by the La–O vector and the plane defined by the water molecule [see Fig. 4(c)].

As La³⁺ is highly charged, it is expected to polarize its surrounding. To assess these effects, we have estimated molecular and ions dipole moments. The molecular charge distribution was studied using maximally localized Wannier functions. These provide an unambiguous way to assign dipole moments to molecules.⁶¹ The dipole moment of water molecules in pure water has been previously estimated with Car–Parrinello molecular dynamics as being on the order of 3.0 D by Silvestrelli and Parrinello.⁶² This value is very close to the value proposed by Badyal *et al.*,⁶³ 2.9 ± 0.6 D, for pure water from an analysis of the experimental x-ray diffraction form-factor. Other theoretical values were also proposed (see, for instance, Refs. 33, 64, and 65).

To further investigate the electronic structure of solvated La³⁺ in water, we have computed the electronic density of states (DOS) of the whole system and the projected density of states (pDOS) on the lanthane atomic states. The DOS for liquid system is the probability density that Kohn–Sham energies are found in an energy range $\epsilon, \epsilon+d\epsilon$. The DOS here was computed similar to previous studies of the electronic structure of pure water^{66,67} as a normalized histogram of the Kohn–Sham energies. The bin width was chosen as 0.05 eV;

TABLE II. Structural properties: distances are in Å and angles in degrees.

	$r_{\text{La-O}}^{(1)}$ ^a	CN ⁽¹⁾ ^b	$r_{\text{La-O}}^{(2)}$ ^a	CN ⁽²⁾ ^b	O-La-O
PP1	2.58 (2.54/2.67)	9.0 (5.2/3.8)	4.8	19	69/135
PP2	2.58 (2.56/2.70)	8.45 (6.27/2.18)	4.7	19.5	71/139
PP3	2.84 (2.81/2.93)	9.16 (6.19/2.97)	4.7	19	69/133/172
P-CLMD ^c	2.52 (2.50/2.58)	9.0 (5.3/3.7)	4.65	18.8	70/137
QM/MM MD ^d	2.65	9.55	5.0	23.4	67/131
MD-Cluster ^e	2.56	8.90	4.68	15.9	...
CPMD ^f	2.52	8.5
EXAFS ^g	2.54	9.20
EXAFS ^h	2.56(2.515/2.64)	9 (6+3)	4.63	18	...
EXAFS ⁱ	2.545	9
EXAFS ^j	2.55(2.52/2.62)	9 (6/3)
XRD ^k	2.57	8	4.7	13	...
XRD ^l	2.58	9.13	5
XRD ^m	2.48	8	4.7

^aFirst ($r_{\text{La-O}}^{(1)}$) and second ($r_{\text{La-O}}^{(2)}$) maximum peak of La-O RDFs (in Å).

^bCoordination number of the first (CN⁽¹⁾) and second (CN⁽²⁾) hydration shells.

^cPolarizable classical MD from Ref. 11.

^dQM/MM MD from Ref. 49.

^eMD on the La(H₂O)₆₀³⁺ cluster from Ref. 48.

^fCPMD with metadynamics and HCTH functional from Ref. 51.

^gEXAFS $L_{\text{II}}-L_{\text{III}}$ -edge from Ref. 68.

^hEXAFS and LAXS L_{II} -edge from Ref. 46.

ⁱEXAFS L_{III} -edge from Ref. 47.

^jEXAFS K-edge from Ref. 8.

^kXRD from Ref. 42.

^lXRD from Ref. 43.

^mXRD from Ref. 44.

a further Gaussian smearing with $\sigma=0.1$ eV was employed to smooth the resulting histograms. The pDOS were obtained by projecting the Kohn–Sham orbitals (occupied and unoccupied) of the whole system on the basis of the pseudoatomic orbitals used to generate the lanthanum pseudopotentials.

III. STRUCTURAL PROPERTIES

Hydration properties are characterized experimentally by La–O distances and first shell coordination numbers. X-ray absorption (EXAFS or X-ray absorption near edge structure) and x-ray diffraction (XRD) experiments are the most common techniques able to shed light on these questions. On La³⁺ hydration, earlier EXAFS and XRD experiments^{8,42–44,46,47,68} report La–O distances in the 2.48–2.56 Å range and first shell coordination number CN=8 or 9. Recently, CN=9 was established as the water coordination number around La³⁺ cation by both experimental and theoretical studies.^{8,46,47,69,70} In evaluating our results, we will first use the acceptable La–O distance range as an indicator of results quality and then the CN, keeping in mind that CN=9 is the major species in the time scale relevant for such experiments.

In Table II, we summarize different structural data on first and second hydration shells as obtained by our CPMD simulations with the three different pseudopotentials developed for the present work (PP1, PP2, and PP3). In the same table, we also show values as obtained from other theoretical and experimental studies and also, for completeness, the old one providing results that are nowadays refined, in particular,

for CN for which experiments are now well established on the value of nine.^{7,8,69} For the first shell, we report the first peak position of the La–O radial distribution function (RDF) and the associated coordination number obtained by integrating this peak. We also report in parenthesis the La–O distances and first shell coordination number (CN⁽¹⁾) obtained by fitting the RDF's first peak with two Gaussian functions. This fitting was done in order to compare our results with new EXAFS data⁸ and our polarizable classical MD simulations.¹¹ Pseudopotentials developed in the present work have to be able to reproduce both La–O distance within the first hydration shell and first shell coordination number of La(III) as established in the literature [i.e., 2.54–2.56 Å range by recent EXAFS experiments⁸ and CN=9 (Refs. 8, 46, and 47)].

As a first result from the CPMD simulations, we can see that the PP3 pseudopotential provides a La–O first hydration shell distance that is too large in comparison to experiments and simulations. The coordination number of 9.16 is about correct, but the error in the La–O distance is too large for this pseudopotential to be considered reliable. Consequently, we do not consider this pseudopotential in the following structural analyses nor obviously in future use.

On the other hand, PP1 and PP2 provide La–O distance in very good agreement with experiments. Coordination numbers are different, in particular PP1 provides CN=9, while PP2 provides an average value of 8.45. This noninteger value arises from a molecular dynamics where a single change in CN is obtained along the trajectory. First 15 ps of the PP2 trajectory provides CN=9, at which point one water molecule from the first hydration shell is lost (goes to the

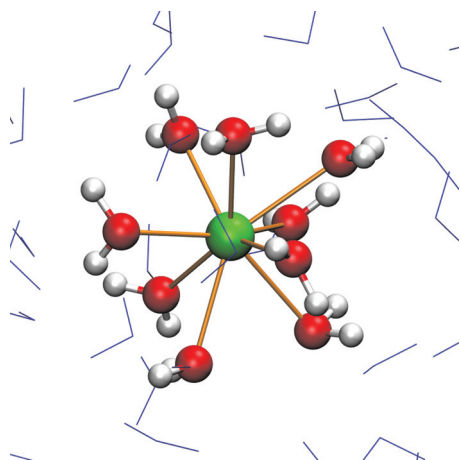


FIG. 1. Snapshot from CPMD simulation of La³⁺ in bulk water. First hydration shell water molecules are shown in ball-and-stick and outer sphere molecules in lines.

second hydration shell), thus providing CN=8 for the rest of the 30 ps trajectory. Note that we do not see any water molecule coming back to the first shell re-establishing the CN=9 structure during the rest of the dynamics. Water exchanges can be very slow with respect to the time length of

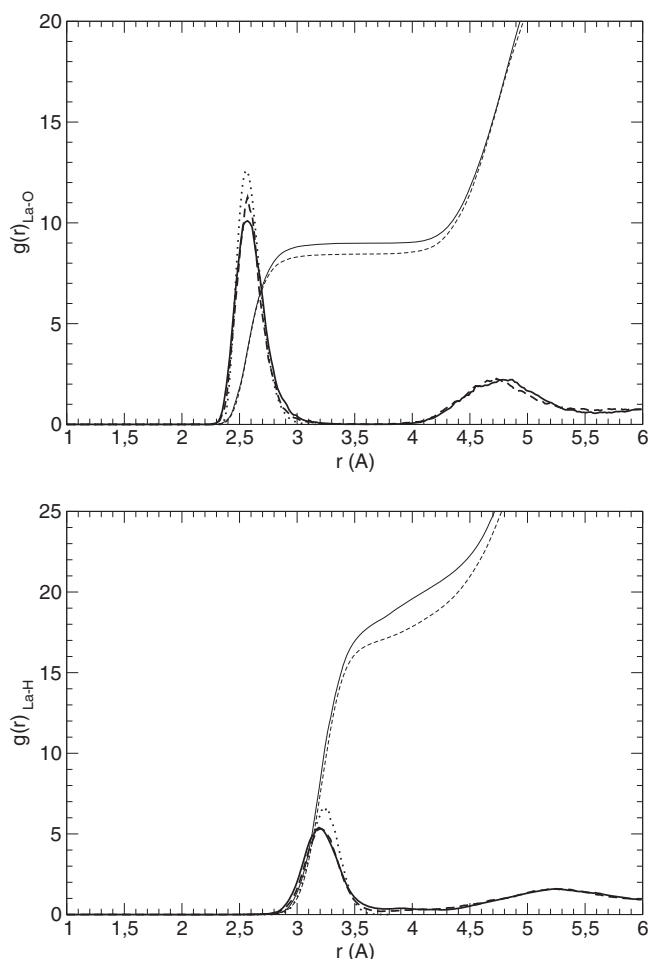


FIG. 2. La–O (upper panel) and La–H (lower panel) radial distribution functions obtained from PP1 (solid line) and PP2 (dashed line) at 300 K. In the dotted lines, we show experimental data from Ref. 71. Also, coordination numbers are shown.

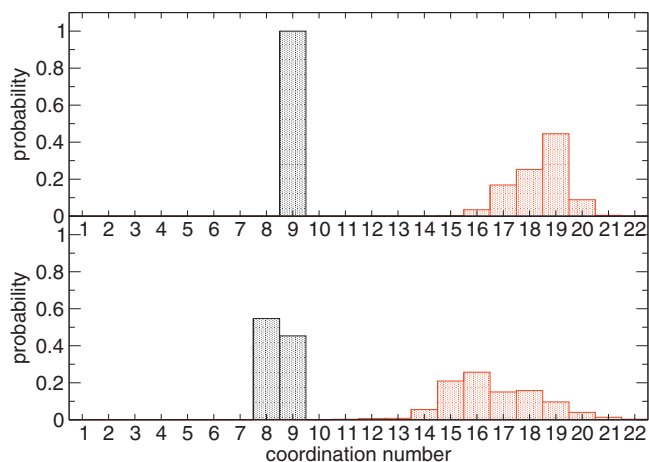


FIG. 3. Probability of finding water molecules in the first and second hydration shells. Upper panel: PP1 results; lower panel: PP2 results.

DFT-based simulations, and it is remarkable that such an exchange has been seen during the PP2 trajectory. The fact that there is a single change from CN=9 to CN=8 during the length of the trajectory and that there is no coming back to CN=9 during the length of the dynamics can be due to a lack in simulation time or from an intrinsic failure in the water-La interaction description due to the pseudopotential. Figure 1 shows a snapshot from the PP1 simulation with nine water molecules in the first hydration shell of La³⁺.

Details on La-water RDF are reported in Fig. 2 where we show La–O and La–H RDF obtained from simulations using both PP1 and PP2. We can see that the first hydration shell is well determined in both cases since the first peak is very sharp and goes to zero before raising up again for the second hydration shell. The La–H RDF does not reach zero exactly—even if very small values are reached—since a hydrogen bonding network is established between first and second shell water molecules. Note that the RDFs reproduce well the experimental positions and also the maximum values obtained by fitting EXAFS experiments⁷¹ that we report in the same Fig. 2. In particular, EXAFS provides a La–O RDF maximum value of about 13 that is slightly higher than the present value of 10–11 and definitely smaller than the value of 15 obtained from polarizable classical MD. As previously found for Co²⁺ in water,²⁵ classical MD tends to overestimate the maximum of RDF, while CPMD has the opposite behavior of providing a smaller value. This reflects the steeper behavior of interaction potential as a function of metal-water distance in classical MD with respect to weaker interactions reported by DFT-based dynamics, as also provided by the typical shift in the vibrational density of states.³⁰

We should pause here in order to discuss possible relationships between our simulation conditions and experimental data. We have one cation in a box of 64 water molecules that was found to be a good compromise between computing time and results reliability for 2+ and 3+ cations.^{25,72,73} In fact, the dependence of RDF peak position with box size can be important below this value,²⁷ while after it, it almost converges.²⁵ Of course, an important point is to have enough sampling (in terms of simulation time) to obtain a good RDF.

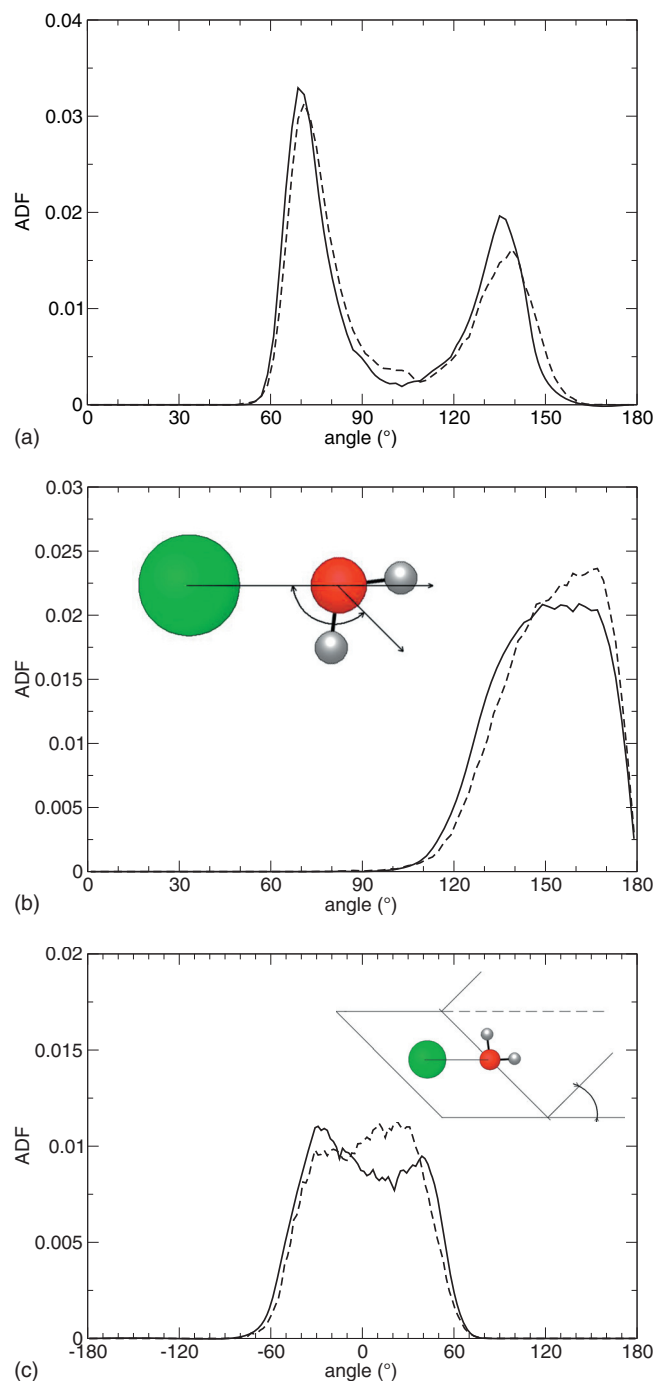


FIG. 4. Angular distribution functions (ADFs) obtained from PP1 (solid lines) and PP2 (dashed lines) simulations. (a) O–La–O, (b) θ angle (as defined in the inset figure), and (c) tilt angle (as defined in the inset).

The 64 water boxes allow us to have quite long simulations in CPMD framework. Classical simulations compared with CPMD simulations on ion hydration have shown that the peak position dependence is almost converged, while, as already remarked, CPMD results tend to provide lower values for RDF at the maximum with respect experiments, corresponding to a more labile metal-water interaction that seems to come from BLYP description. Further, one can question about La(III) concentration we simulate. In principle, studying one cation in pure water with PBC should correspond to ideal dilution conditions. Deviations come from box dimen-

sions and possible unphysical La–La correlations. Thus, the studies of results convergence with respect to box size are the typical way of estimate that. Moreover, often experiments are interpreted in the spirit of infinite dilution and compared with corresponding simulations.^{10,74–76} The role of counterions, at high concentration, on Ln(III) solvation was found to be important and interesting by both theoretical^{54,77,78} and experimental sides,⁷⁹ pointing out an important role when moving to concentrate solutions. Here, we are not interested in such effects, and we keep, as in many experimental interpretations, the limit of infinite dilution (i.e., no role of counterions on structure). The good agreement with respect to such experiments at low concentration is a good sign of the reliability of our simulation conditions.

The coordination number (CN) is displayed with respect to the La–O distance in the figure and provides a plateau region of CN=9 in the first hydration shell in the case of PP1 and about 8.45 in the case of PP2. In Fig. 3, we show the probability of finding N water molecules in the first and second hydration shell for both pseudopotentials. In the case of PP1 simulations, we found always 9 water molecules in the first hydration shell, in agreement with recent experiments^{8,46} and theoretical calculations^{11,70} for which CN=9 is the prevalent species. The second hydration shell is, as usual, less well defined, and we have a certain variation in the number of water molecules. The two most abundant numbers of water molecules in the second hydration shell are 18 (two times the number of water molecules in the first shell) and 19. Experimentally, no clear information is present on the second hydration shell, but our values are similar to what was found in other simulations and deduced from certain experiments.^{11,46} Simulations done with PP2 present a different picture of the first hydration shell since we can see two coordination numbers of 9 and 8, which reflect the change in CN at about midtrajectory discussed above. Note that CN = 8.5 was also found in metadynamics simulations done with the HCTH functional and a similar semicore pseudopotential.⁵¹ On the other hand, the PP1 pseudopotential is able to provide the correct La–O distance and CN (at least on the simulation time length), thus strengthening the view that a good choice of pseudopotential is crucial to correctly describe the metal-solvent interaction. Note also that the fictitious mass employed in the Car–Parrinello dynamics framework has a crucial role on the final value of CN. Hence the use of higher values of the fictitious mass together with the PP1 pseudopotential lead to the loss of one water molecule in the first shell of La(III), thus giving rise to a CN = 8 hydration structure.

To characterize in more details the organization of the nine water molecules around the central metal atom, we employ the O–La–O angular distribution function (ADF), reported in Fig. 4(a). This ADF shows two peaks at about 70° and 135° that correspond to the trigonal tricapped prism structure as pointed out by previous studies.^{11,13,14} The curve corresponding to PP1, for which we have CN=9 for the whole simulation run, clearly shows only two peaks, while the simulation done using the PP2 has a signal that includes the coexistence of the two CN=9 and CN=8 stoichiometries.

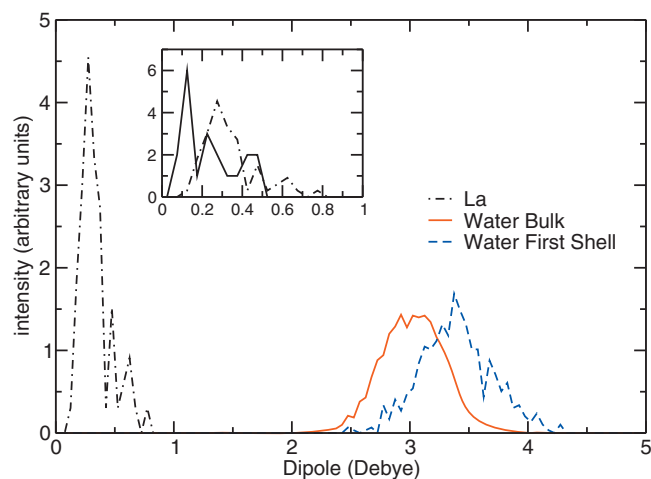


FIG. 5. Dipole distribution function on bulk water molecules (solid line), first hydration shell water molecules (dashed line), and La (dot-dashed line). In the inset, we show La dipoles obtained with PP1 (dot-dashed line) and PP2 (solid line).

The sampling is not enough to have a statistically representative signal, but we can see that the two peaks are systematically shifted toward slightly higher values and a new peak seems to be present around 100° – 110° . This feature is common to CN=8 structures,^{13,14} where the supplementary peak corresponds more to a trigonal dodecahedron structure than to a square-antiprism one.

From trajectory analysis, we can study how first shell water molecules are spatially distributed around the metal cation by means of two angular distribution functions: (i) the θ angle [Fig. 4(b)] that is the angle between the O–La vector and the vector resulting from the sum of the O–H bonds and (ii) the tilting angle [Fig. 4(c)] formed between the La–O vector and the plane defined by the water molecule. The tilting angle is, as expected, centered at 0° with an almost symmetric shape reaching zero at about $\pm 60^{\circ}$. This shows a high degree of flexibility of first shell water molecules that was already pointed out for La(III) (Ref. 49) and other cations such as Cu(II) (Ref. 80) and Zn(II) (Ref. 81) (even if less pronounced) but is atypical for instance for a smaller trivalent cation like Al(III).⁸² This property does not seem to be dependent on the coordination number of the metal but mainly due to the metal-water and water-water interactions in the first shell that are to a large extent dependent on the polarization induced by the cation. The θ angular distribution also shows this feature, with a peak at about 160° (PP1)– 170° (PP2) and a long tail. Note that the signal suffers also from a lack in statistics due to the time scale accessible from CPMD simulations that is, even in the present study of 30 ps long simulations, small with respect to characteristic solvent dynamics time scales.

IV. ELECTRONIC PROPERTIES

DFT-based simulations treat explicitly valence electrons when determining interaction energies, such that we can analyze the obtained wave functions in liquid phase and make a connection between electronic properties and hydration properties.

In Fig. 5 we present the dipole moments on La(III), on the water molecules from the first hydration shell of La(III) and on the water molecules from the remaining bulk. The highly charged La³⁺ cation significantly polarizes the water molecules in its first hydration shell. These water molecules acquire on average a dipole moment of about 0.5 D higher than the water molecules in the bulk. Note that results on water dipole moment, bulk or first shell, are not dependent on the PP used; thus here we report only those obtained from PP1. Such a polarization has also been found in the case of other lanthanoids(III) immersed in liquid water.¹⁵ The dipole moment for bulk water molecules is similar to pure liquid water with a mean dipole peaked around 3 D.⁶² The large difference in dipole of first shell and bulk water molecules clearly explains the fact that, as was empirically shown in the framework of classical molecular dynamics of lanthanoid(III) hydration, water polarizability must be taken into account in order to better reproduce structural and dynamical properties.⁸³

The lanthanum cation itself gets also polarized with an approximate dipole around 0.2–0.3 D, as obtained in PP1 simulations. This shows that although highly charged, its polarizability arising from the eight semicore electrons $5s$ and $5p$ cannot be neglected. Note that these values are in agreement with a previous study of the solvation of La³⁺ in highly concentrated LiCl aqueous solutions.⁵⁴ In the same figure (inset), we compare the La³⁺ dipole obtained from PP1 with that obtained from PP2. We should note that in average PP2, providing a smaller CN, gives a smaller dipole and thus a more compact cation. This is in agreement with the known phenomenon in the lanthanoid series, such that a decreasing in atomic radius and polarizability corresponds to a decrease in coordination number.^{8,14}

Figure 6 displays the DOS (density of states) and pDOS (projected density of states) of the full system (La³⁺ and water molecules), where the zero corresponds to the Fermi level. While valence occupied La³⁺ orbitals, $5s$ and $5p$, are well distinct from liquid water “bands”—that is, dominating but not *per se* interesting in this study—the $4f$ and $5d$ orbitals are unoccupied, being situated well above the Fermi level, and have energies similar to unoccupied orbitals of water, and thus we might expect some mixing. Note that here we employ the concept of “water band structure” and DOS for an aperiodic system as in Prendergast *et al.*,⁶⁷ which gives information about electronic structure of the liquid. The two pseudopotentials provide similar DOS and pDOS. The main difference resides in the fact that PP2 seems to provide some bimodal peaks. By inspecting the different snapshots producing them, we noticed that this shape does not come from an orbital splitting of individual snapshots but from a larger band mobility due to dynamics. This means that using PP2, La³⁺ orbitals have more difficulty in adapting themselves as a function of water dynamics, while by using PP1, these orbitals are individually broader, with a resulting larger dipole moment, as noticed before. As for the unoccupied orbitals of La³⁺, the $4f$ orbitals are found lower in energy than the $5d$ orbitals, also in the case of PP2 where the overlap comes from the different snapshots and not from a real overlap noticed on individual configurations. To the best

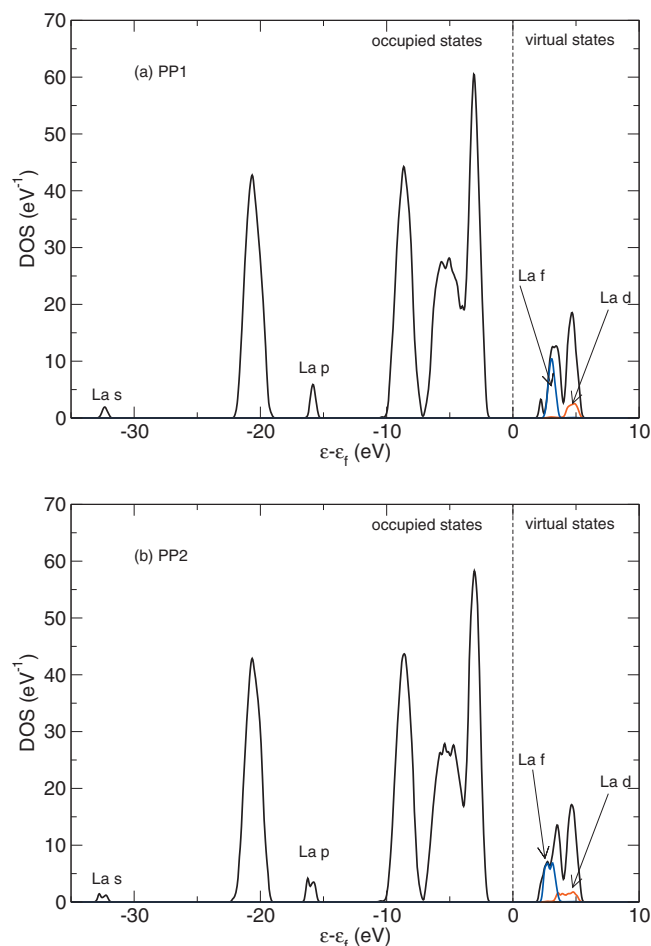


FIG. 6. Density of states (DOS) and projected DOS on the Lanthanum pseudoatomic orbitals. The zero corresponds to the Fermi level. (a) PP1 simulations. (b) PP2 simulations.

of our knowledge, there are no data in the literature to directly compare this f - d gap to (experiments and simulations). The best relevant comparison can be done with the DFT calculations of $\text{Ce}^{3+}-(\text{H}_2\text{O})_9$,⁸⁴ the next cation in the lanthanoid series, where the supplementary electron occupies the $4f$ orbital, being lower in energy than $5d$. Of course, when the La^{3+} cation is subjected to stronger ligand fields, a stabilization of the d orbitals can be observed.^{85–87} By inspecting differences between DOS and pDOS (a small difference corresponds to a small coupling with water orbitals) and isocountour plots,⁸⁸ shown in Fig. 7, for f and d orbitals, we can notice that $4f$ orbitals are decoupled from water orbitals, while $5d$ orbitals are mixed with those of water. All together, the $5s$, $5p$, and $4f$ orbitals of $\text{La}(\text{III})$ are highly decoupled from the solvent and can be seen as not “easily accessible,” which suggests that La^{3+} is nonreactive and it is a hard ion in the hard and soft acid base frameworks.⁴¹ This is indeed expected for such a highly charged and compact ion. The other valuable information from the electronic investigation is that the La^{3+} -water interaction is mainly electrostatic.

Finally, the small size of the $4f$ orbitals also leads to a small ligand field splitting. For an ideal tricapped bipyramid of D_{3h} symmetry, one expects $a'_1 \oplus a'_2 \oplus a'_2 \oplus e' \oplus e''$ splitting of the energy levels of the f band (see Table III). No such splitting of the $4f$ band is visible on the pDOS, which points

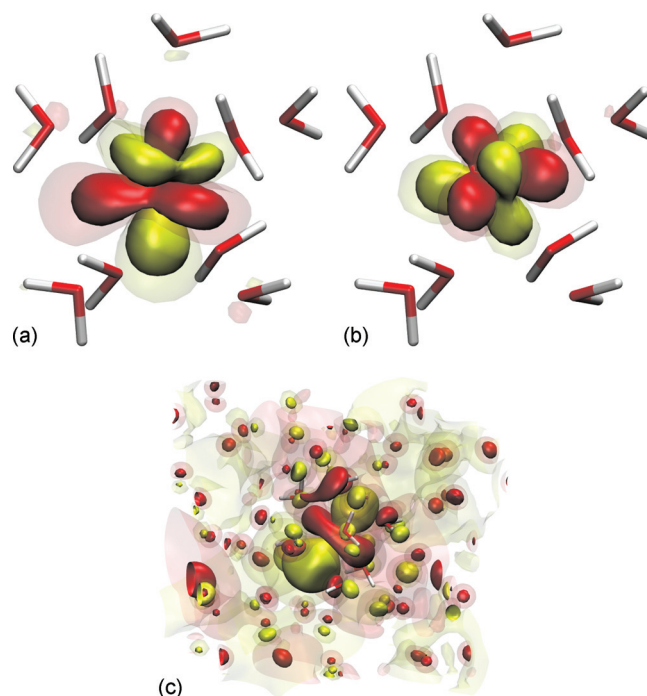


FIG. 7. Snapshots of Kohn-Sham orbitals. (a) and (b) are f -like orbitals at $\epsilon_f = 2.80$ eV and $\epsilon_f = 2.84$ eV, respectively. The light isocontours correspond to 95% of the orbital probability, and the darker isocontours correspond to 90% of the orbital probability. (c) is a d -like orbital ($\epsilon_f = 4.25$ eV), where the light isocontours correspond to 90% of the orbital probability total charge and the darker isocontours correspond to 50% of the orbital probability.

toward a ligand field splitting lower than the broadening due to thermal fluctuations. For $\text{Gd}^{3+}(\text{H}_2\text{O})_8$ in D_{4d} symmetry, the ligand field splitting of the $4f$ orbitals has been predicted to be of the order of 0.1 eV.⁸⁹ This is indeed significantly smaller than the thermal broadening, which is about 0.5 eV as estimated from the width of the $5s$, $5p$, and $4f$ bands corresponding to $\text{CN}=9$ [Fig. 6(a)] and even bigger for structures providing $\text{CN}=8$ [Fig. 6(b)]. We can thus conclude that there is not a clear signature of water molecules on the $4f$ band. Similarly, the geometry of water molecules coordinated to La^{3+} does not seem to be specially imposed by the actually empty $4f$ and $5d$ orbitals. This is consistent with the fact that the d element Y^{3+} has a hydration structure similar to those of the heavy lanthanoids(III) Tb^{3+} and Er^{3+} .^{90,91}

V. CONCLUSIONS

In this paper, we report first-principle molecular dynamics simulations of La^{3+} in bulk liquid water that are able to reproduce structural properties of this system. This includes not only the La-water distance in the first hydration shell but also a stable coordination number equal to nine for the time spanned by the simulation. To that end, three pseudopotentials have been developed and tested, and we found that the one using $\text{La}(\text{III})$ as reference state is the most accurate. A small fictitious electronic mass, able to keep the Car-Parrinello dynamics close enough to the Born-Oppenheimer surface, is also necessary to correctly reproduce hydration properties.

The large charge of La^{3+} is shown to strongly polarize the water molecules located in the first hydration shell of the

TABLE III. Irreducible decomposition of the f orbitals according to the D_{3h} symmetry. For each conjugacy class \bar{s} , the image of the f orbitals by the representant s of that class is exhibited.

Orbitals	\bar{E}	\bar{C}_3	\bar{C}_2	$\bar{\sigma}_h$	\bar{S}_3	$\bar{\sigma}_v$	Irrep.
$f_{x(x^2-3y^2)}$	$f_{x(x^2-3y^2)}$	$f_{x(x^2-3y^2)}$	$f_{x(x^2-3y^2)}$	$f_{x(x^2-3y^2)}$	$f_{x(x^2-3y^2)}$	$f_{x(x^2-3y^2)}$	a'_1
$f_{y(3x^2-y^2)}$	$f_{y(3x^2-y^2)}$	$f_{y(3x^2-y^2)}$	$-f_{y(3x^2-y^2)}$	$f_{y(3x^2-y^2)}$	$f_{y(3x^2-y^2)}$	$-f_{y(3x^2-y^2)}$	a'_2
f_{z^3}	f_{z^3}	f_{z^3}	$-f_{z^3}$	$-f_{z^3}$	$-f_{z^3}$	f_{z^3}	a''_2
$\begin{pmatrix} f_{xz^2} \\ f_{yz^2} \end{pmatrix}$	$\begin{pmatrix} f_{xz^2} \\ f_{yz^2} \end{pmatrix}$	$\begin{pmatrix} -\frac{1}{2}f_{xz^2} + \frac{\sqrt{3}}{2}f_{yz^2} \\ -\frac{\sqrt{3}}{2}f_{xz^2} - \frac{1}{2}f_{yz^2} \end{pmatrix}$	$\begin{pmatrix} f_{xz^2} \\ -f_{yz^2} \end{pmatrix}$	$\begin{pmatrix} f_{xz^2} \\ f_{yz^2} \end{pmatrix}$	$\begin{pmatrix} -\frac{1}{2}f_{xz^2} + \frac{\sqrt{3}}{2}f_{yz^2} \\ -\frac{\sqrt{3}}{2}f_{xz^2} - \frac{1}{2}f_{yz^2} \end{pmatrix}$	$\begin{pmatrix} f_{xz^2} \\ -f_{yz^2} \end{pmatrix}$	e'
$\begin{pmatrix} f_{xyz} \\ f_{(x^2-y^2)z/2} \end{pmatrix}$	$\begin{pmatrix} f_{xyz} \\ f_{(x^2-y^2)z/2} \end{pmatrix}$	$\begin{pmatrix} -\frac{1}{2}f_{xyz} + \frac{\sqrt{3}}{2}f_{(x^2-y^2)z/2} \\ -\frac{\sqrt{3}}{2}f_{xyz} - \frac{1}{2}f_{(x^2-y^2)z/2} \end{pmatrix}$	$\begin{pmatrix} f_{xyz} \\ -f_{(x^2-y^2)z/2} \end{pmatrix}$	$\begin{pmatrix} -f_{xyz} \\ -f_{(x^2-y^2)z/2} \end{pmatrix}$	$\begin{pmatrix} \frac{1}{2}f_{xyz} - \frac{\sqrt{3}}{2}f_{(x^2-y^2)z/2} \\ \frac{\sqrt{3}}{2}f_{xyz} + \frac{1}{2}f_{(x^2-y^2)z/2} \end{pmatrix}$	$\begin{pmatrix} -f_{xyz} \\ f_{(x^2-y^2)z/2} \end{pmatrix}$	e''

ion by about 0.5 D. The shift of dipoles between first shell and bulk water molecules found here is of the same order of magnitude as the one found for other lanthanoids(III),¹⁵ such as Nd³⁺, Gd³⁺, and Yb³⁺, as obtained from classical molecular dynamics with a polarizable force-field. Our DFT-based study then justifies from an electronic structure point of view the need of using polarizable classical force-fields for studying the solvation of La³⁺ in liquid water. Furthermore, the inspection of the electronic state of La³⁺ in water shows that although the cation itself is also polarized by the solvent electric field by about 0.5 D, it can be considered as a hard cation with very little involvement with the lanthanum orbitals in the interaction with the surrounding water. The compact f orbitals hybridize only minimally with water orbitals, while the d orbitals, found here to be within DFT slightly of higher energy, have noticeable hybridization with water orbitals. However, these orbitals are unoccupied and thus do not participate to bonding.

It is essential to have at our disposal an accurate pseudo-potential for La³⁺ and setup for first-principle Car–Parrinello molecular dynamics simulations, as provided by the present work. Investigations of the aqueous chemistry of La³⁺, for instance, hydrolysis, and the aqueous complexation of La³⁺ with ligands typically of interest in the context of nuclear storage, including the chemical reactivity competition between the ligand protonation and the ligand-metal complexation, can be envisaged with DFT-MD simulations using the protocol tested in this work. Our research interests are indeed going into these directions.

ACKNOWLEDGMENTS

This work was granted access to the HPC resources of IDRIS and CCRT under the allocation (Grant No. x2009071870) made by GENCI (Grand Equipement National de Calcul Intensif) in France. C.T. acknowledges an internship funding from CEA-DEN.

- ¹H. Ohtaki and T. Radnai, *Chem. Rev. (Washington, D.C.)* **93**, 1157 (1993).
- ²Y. Marcus, *Chem. Rev. (Washington, D.C.)* **88**, 1475 (1988).
- ³G. Johansson, *Adv. Inorg. Chem.* **187**, 151 (1992).
- ⁴T. S. Hofer, H. T. Train, C. F. Schwenk, and B. M. Rode, *J. Comput. Chem.* **25**, 211 (2003).
- ⁵F. P. Rotzinger, *Chem. Rev. (Washington, D.C.)* **105**, 2003 (2005).
- ⁶C. Cossy, L. Helm, D. H. Powell, and A. E. Merbach, *New J. Chem.* **19**, 27 (1995).
- ⁷L. Helm and A. E. Merbach, *Chem. Rev. (Washington, D.C.)* **105**, 1923 (2005).
- ⁸I. Persson, P. D'Angelo, S. De Panfilis, M. Sandstrom, and L. Eriksson, *Chem.-Eur. J.* **14**, 3056 (2008).
- ⁹M. Duvaill, R. Spezia, and P. Vitorge, *ChemPhysChem* **9**, 693 (2008).
- ¹⁰P. D'Angelo, A. Zitolo, V. Migliorati, G. Mancini, I. Persson, and G. Chillemi, *Inorg. Chem.* **48**, 10239 (2009).
- ¹¹M. Duvaill, M. Souaille, R. Spezia, T. Cartailier, and P. Vitorge, *J. Chem. Phys.* **127**, 034503 (2007).
- ¹²C. Clavaguera, F. Calvo, and J.-P. Dognon, *J. Chem. Phys.* **124**, 074505 (2006).
- ¹³T. Kowall, F. Foglia, L. Helm, and A. E. Merbach, *J. Phys. Chem.* **99**, 13078 (1995).
- ¹⁴M. Duvaill, P. Vitorge, and R. Spezia, *J. Chem. Phys.* **130**, 104501 (2009).
- ¹⁵A. Villa, B. Hess, and H. Saint-Martin, *J. Phys. Chem. B* **113**, 7270 (2009).
- ¹⁶F. M. Floris and A. Tani, *J. Chem. Phys.* **115**, 4750 (2001).
- ¹⁷M. F. Bush, R. J. Saykally, and E. R. Williams, *J. Am. Chem. Soc.* **130**, 9122 (2008).
- ¹⁸D. L. Clark, D. E. Hobart, and M. P. Neu, *Chem. Rev. (Washington, D.C.)* **95**, 25 (1995).
- ¹⁹T. Vercouter, P. Vitorge, B. Amekraz, E. Giffaut, S. Hubert, and C. Moulin, *Inorg. Chem.* **44**, 5833 (2005).
- ²⁰T. Vercouter, B. Amekraz, C. Moulin, E. Giffaut, and P. Vitorge, *Inorg. Chem.* **44**, 7570 (2005).
- ²¹V. Philippini, T. Vercouter, J. Aupiais, S. Topin, C. Ambard, A. Chaussé, and P. Vitorge, *Electrophoresis* **29**, 2041 (2008).
- ²²R. Car and M. Parrinello, *Phys. Rev. Lett.* **55**, 2471 (1985).
- ²³L. Bernasconi, J. Blumberger, M. Sprik, and R. Vuilleumier, *J. Chem. Phys.* **121**, 11885 (2004).
- ²⁴R. Ayala and M. Sprik, *J. Chem. Theory Comput.* **2**, 1403 (2006).
- ²⁵R. Spezia, M. Duvaill, P. Vitorge, T. Cartailier, J. Tortajada, P. D'Angelo, and M.-P. Gaigeot, *J. Phys. Chem. A* **110**, 13081 (2006).
- ²⁶M. Bühl, S. Grigoleit, H. Kabrede, and F. T. Mauschick, *Chem.-Eur. J.* **12**, 477 (2006).
- ²⁷S. Amira, D. Spangberg, V. Zelin, M. Probst, and K. Hermansson, *J. Phys. Chem. B* **109**, 14235 (2005).

- ²⁸O. V. Yazyev and L. Helm, *Theor. Chem. Acc.* **115**, 190 (2006).
- ²⁹A. J. Sillanpää, R. Aksela, and K. Laasonen, *Phys. Chem. Chem. Phys.* **5**, 3382 (2003).
- ³⁰R. Spezia, C. Bresson, C. Den Auwer, and M.-P. Gaigeot, *J. Phys. Chem. B* **112**, 6490 (2008).
- ³¹A. D. Becke, *Phys. Rev. A* **38**, 3098 (1988).
- ³²C. Lee, W. Yang, and R. G. Parr, *Phys. Rev. B* **37**, 785 (1988).
- ³³K. Laasonen, M. Sprik, M. Parrinello, and R. Car, *J. Chem. Phys.* **99**, 9080 (1993).
- ³⁴J. VandeVondele, F. Mohamed, M. Krack, J. Hutter, M. Sprik, and M. Parrinello, *J. Chem. Phys.* **122**, 014515 (2005).
- ³⁵D. Marx, J. Hutter, and M. Parrinello, *Chem. Phys. Lett.* **241**, 457 (1995).
- ³⁶M. E. Tuckerman, K. Laasonen, M. Sprik, and M. Parrinello, *J. Phys. Chem.* **99**, 5749 (1995).
- ³⁷P. Hunt and M. Sprik, *ChemPhysChem* **6**, 1805 (2005).
- ³⁸J. M. Heuft and E. J. Meijer, *J. Chem. Phys.* **122**, 094501 (2005).
- ³⁹J. M. Heuft and E. J. Meijer, *J. Chem. Phys.* **123**, 094506 (2005).
- ⁴⁰J. M. Heuft and E. J. Meijer, *J. Chem. Phys.* **119**, 11788 (2003).
- ⁴¹R. Vuilleumier and M. Sprik, *J. Chem. Phys.* **115**, 3454 (2001).
- ⁴²G. Johansson and H. Wakita, *Inorg. Chem.* **24**, 3047 (1985).
- ⁴³A. Habenschuss and F. H. Spedding, *J. Chem. Phys.* **70**, 2797 (1979).
- ⁴⁴L. S. Smith and D. L. Wertz, *J. Am. Chem. Soc.* **97**, 2365 (1975).
- ⁴⁵J. A. Solera, J. Garcia, and M. G. Proietti, *Phys. Rev. B* **51**, 2678 (1995).
- ⁴⁶J. Näslund, P. Lindqvist-Reis, I. Persson, and M. Sandström, *Inorg. Chem.* **39**, 4006 (2000).
- ⁴⁷S.-I. Ishiguro, Y. Umebayashi, K. Kato, R. Takahashib, and K. Ozutsumi, *J. Chem. Soc., Faraday Trans.* **94**, 3607 (1998).
- ⁴⁸C. Clavaguéra, R. Pollet, J. M. Soudan, V. Brenner, and J. P. Dognon, *J. Phys. Chem. B* **109**, 7614 (2005).
- ⁴⁹T. S. Hofer, H. Scharnagl, B. R. Randolph, and B. M. Rode, *Chem. Phys.* **327**, 31 (2006).
- ⁵⁰O. V. Yazyev and L. Helm, *J. Chem. Phys.* **127**, 084506 (2007).
- ⁵¹T. Ikeda, M. Hirata, and T. Kimura, *J. Chem. Phys.* **122**, 244507 (2005).
- ⁵²A. V. Astashkin, A. M. Raitsimring, and P. Caravan, *J. Phys. Chem. A* **108**, 1990 (2004).
- ⁵³A. M. Raitsimring, A. V. Astashkin, D. Baute, D. Goldfarb, and P. Caravan, *J. Phys. Chem. A* **108**, 7318 (2004).
- ⁵⁴L. Petit, R. Vuilleumier, P. Maldivi, and C. Adamo, *J. Phys. Chem. B* **112**, 10603 (2008).
- ⁵⁵N. Troullier and J. L. Martins, *Phys. Rev. B* **43**, 1993 (1991).
- ⁵⁶L. Kleinman and D. M. Bylander, *Phys. Rev. Lett.* **48**, 1425 (1982).
- ⁵⁷J. Hutter, A. Alavi, T. Deutsch, M. Bernasconi, S. Goedecker, D. Marx, M. Tuckerman, and M. Parrinello, CPMD, version 3.9.1, IBM Research Division, IBM Corp and Max Planck Institute Stuttgart, 2004.
- ⁵⁸S. Nosé, *J. Chem. Phys.* **81**, 511 (1984).
- ⁵⁹S. Nosé, *Mol. Phys.* **52**, 255 (1984).
- ⁶⁰W. G. Hoover, *Phys. Rev. A* **31**, 1695 (1985).
- ⁶¹M.-P. Gaigeot and M. Sprik, *J. Phys. Chem. B* **107**, 10344 (2003).
- ⁶²P. L. Silvestrelli and M. Parrinello, *Phys. Rev. Lett.* **82**, 3308 (1999).
- ⁶³Y. S. Badyal, M.-L. Saboungi, D. L. Price, S. D. Shastri, D. R. Haefner, and A. K. Soper, *J. Chem. Phys.* **112**, 9206 (2000).
- ⁶⁴E. R. Batista, S. S. Xantheas, and H. Jonsson, *J. Chem. Phys.* **109**, 4546 (1998).
- ⁶⁵F.-X. Coudert, R. Vuilleumier, and A. Boutin, *ChemPhysChem* **7**, 2464 (2006).
- ⁶⁶P. Hunt, M. Sprik, and R. Vuilleumier, *Chem. Phys. Lett.* **376**, 68 (2003).
- ⁶⁷D. Prendergast, J. C. Grossman, and G. Galli, *J. Chem. Phys.* **123**, 014501 (2005).
- ⁶⁸P. Allen, J. J. Bucher, D. K. Shuh, N. M. Edelstein, and I. Craig, *Inorg. Chem.* **39**, 595 (2000).
- ⁶⁹P. D'Angelo, A. Zitolo, V. Migliorati, and I. Persson, *Chem.-Eur. J.* **16**, 684 (2010).
- ⁷⁰V. Buzko, I. Sukhno, and M. Buzko, *Int. J. Quantum Chem.* **107**, 2353 (2007).
- ⁷¹M. Duvail, P. D'Angelo, M.-P. Gaigeot, P. Vitorge, and R. Spezia, *Radiochim. Acta* **97**, 339 (2009).
- ⁷²E. Bylaska, M. Valiev, J. Rustad, and J. Weare, *J. Chem. Phys.* **126**, 104505 (2007).
- ⁷³S. Bogatko, E. Bylaska, and J. Weare, *J. Phys. Chem. A* **114**, 2189 (2010).
- ⁷⁴P. D'Angelo, V. Barone, G. Chillemi, N. Sanna, W. Mayer-Klauke, and N. Pavel, *J. Am. Chem. Soc.* **124**, 1958 (2002).
- ⁷⁵G. Chillemi, P. D'Angelo, N. Pavel, N. Sanna, and V. Barone, *J. Am. Chem. Soc.* **124**, 1968 (2002).
- ⁷⁶P. D'Angelo, V. Migliorati, G. Mancini, V. Barone, and G. Chillemi, *J. Chem. Phys.* **128**, 084502 (2008).
- ⁷⁷W. Meier, P. Bopp, M. M. Probst, E. Spohr, and J. L. Lin, *J. Phys. Chem.* **94**, 4672 (1990).
- ⁷⁸M. Duvail, A. Ruas, L. Venault, P. Moisy, and P. Guilbaud, *Inorg. Chem.* **49**, 519 (2010).
- ⁷⁹L. Soderholm, S. Skanthakumar, and R. Wilson, *J. Phys. Chem. A* **113**, 6391 (2009).
- ⁸⁰C. F. Schwenk and B. M. Rode, *J. Chem. Phys.* **119**, 9523 (2003).
- ⁸¹M. Q. Fatmi, T. S. Hofer, B. R. Randolph, and B. M. Rode, *J. Chem. Phys.* **119**, 4514 (2005).
- ⁸²T. S. Hofer, B. R. Randolph, and B. M. Rode, *Phys. Chem. Chem. Phys.* **7**, 1382 (2005).
- ⁸³T. Kowall, F. Foglia, L. Helm, and A. E. Merbach, *J. Am. Chem. Soc.* **117**, 3790 (1995).
- ⁸⁴A. Dinescu and A. E. Clark, *J. Phys. Chem. A* **112**, 11198 (2008).
- ⁸⁵C. Adamo and P. Maldivi, *J. Phys. Chem. A* **102**, 6812 (1998).
- ⁸⁶L. Maron and O. Eisenstein, *J. Phys. Chem. A* **104**, 7140 (2000).
- ⁸⁷C. Clavaguera, J. P. Dognon, and P. Pyykko, *Chem. Phys. Lett.* **429**, 8 (2006).
- ⁸⁸M. Haranczyk and M. Gutowski, *J. Chem. Theory Comput.* **4**, 689 (2008).
- ⁸⁹A. Borel, L. Helm, and C. A. E. Daul, *Chem. Phys. Lett.* **383**, 584 (2004).
- ⁹⁰S. Díaz-Moreno, A. Munoz-Paez, and J. Chaboy, *J. Phys. Chem. A* **104**, 1278 (2000).
- ⁹¹S. Ramos, G. W. Neilson, A. C. Barnes, and A. Mazuelas, *J. Phys. Chem. B* **105**, 2694 (2001).